第 24 卷第 5 期
2008 年 5 月

无 机 化 学 学 报
CHINESE JOURNAL OF INORGANIC CHEMISTRY

Vol.24 No.5
818~822

研究简报

$CeOHCO_3$ 和 CeO_2 束状纳米结构的制备及表征

张晓娟 张胜义* 田玉鹏 金葆康 吴杰颖
(安徽大学化学化工学院,合肥 230039)

关键词: $CeOHCO_3$; CeO_2; 液相合成法; 光学性质
中图分类号: O614.33+2 **文献标识码**: A **文章编号**: 1001-4861(2008)05-0818-05

Preparation and Characterization of Crystalline $CeOHCO_3$ and CeO_2 with Bundle-like Nanostructures

ZHANG Xiao-Juan ZHANG Sheng-Yi* TIAN Yu-Peng JIN Bao-Kang WU Jie-Ying
(*College of Chemistry and Engineering, Anhui University, Hefei* 230039)

Abstract: The cantaloupe-like particles of $CeOHCO_3$ were synthesized in aqueous solution by using cetyltrimethylammonium bromide (CTAB) as soft template. Then, the bunchiness rods of CeO_2 were obtained by calcining $CeOHCO_3$ at 450 ℃. The results of thermogravimetric/differential thermal analysis reveal that an endothermic reaction with decomposition is involved in the transformation process from $CeOHCO_3$ to CeO_2. By scanning electron microscopy and X-ray diffraction analysis, it is found that the orthorhombic phase $CeOHCO_3$ particles are constituted of short nanorods with diameters ranging from several tens nm to over 100 nm, and the cubic phase CeO_2 rods are composed of small particles with diameter ca. 15 nm. From the results of UV-Vis absorption and photoluminescence analysis, it is found that the CeO_2 possess abundant defects, and the band gaps of the CeO_2 and $CeOHCO_3$ are *ca.* 2.70 eV and 3.87 eV, respectively.

Key words: $CeOHCO_3$; CeO_2; solution route; optical property

0 Introduction

Nanomaterials have drawn increasing interests due to their novel characteristics and broad applications. As well-known, the size and morphology of nanomaterials strongly affect the properties of the nanomaterials, therefore, many research efforts have been devoted to the design and synthesis of nanomaterials with a given structure. Ceria (CeO_2), a rare earth compound, has received much attention for its particular properties and applications[1~4]. For example, CeO_2 nanoparticles can be used as automobile exhaust catalysts, electrode component in fuel-cells, glass-polishing materials, ultraviolet absorbent, photoluminescence materials, ceramic additives and so on[5~12]. Since Matijevic and co-workers[13] synthesized CeO_2 nanoparticles in 1987, a number of methods for the synthesis of CeO_2 nanostructures have been reported, such as hydrothermal synthesis[10,14~17], chemical vapor deposition[18], porous polymeric template synthesis[19], surfactant-assisted synthesis[20], and reverse micelle synthesis[21]. In this paper, a simple surfactant-assisted method for the synthesis of

收稿日期:2008-01-12。收修改稿日期:2008-03-18。
国家自然科学基金(No.20775001,50532030,20771001),安徽省基金(No.050440702,2006KJ007TD)资助项目。
*通讯联系人。E-mail:syzhangi@126.com
第一作者:张晓娟,女,24 岁,硕士研究生;研究方向:纳米合成化学。

$CeOHCO_3$ and CeO_2 nanostructures, is presented. In synthesis, the cantaloupe-like particles of $CeOHCO_3$ were prepared in aqueous solution by using cetyltrimethylammonium bromide (CTAB) as the soft template. Then, the bunchiness rods of CeO_2 were obtained by calcining $CeOHCO_3$. The results show that the orthormbic phase $CeOHCO_3$ particles are constituted of short nanorods, and the cubic phase CeO_2 rods are composed of small particles. In addition, the optical properties of both $CeOHCO_3$ and CeO_2 were studied by UV-Vis absorption and photoluminescence analysis.

1 Experimental

1.1 Synthesis

The reagents were all of analytical grade and were used without further purification. In a typical synthesis process, 0.60 g CTAB and 0.43 g $Ce(NO_3)_3 \cdot 6H_2O$ were first dissolved in 15 mL deionized water under stirring. Then, the reaction was started up by adding 2.7 g urea ($CO(NH_2)_2$) into the mixture solution. After stirring for 40 min, the solution was kept in water bath at 95℃ for 8 h. The white precipitate formed in reaction solution was filtered out, washed with deionized water and dried under infrared light. Finally, the yellow powder was obtained by calcining the white precipitate at 450 ℃ for 1 h.

1.2 Characterization

The as-obtained products were characterized by scanning electron microscopy (SEM, 1530 VP Ger. LEO), X-ray diffraction (XRD, Japan Rigaku D/max-RA X-ray diffractometer, with graphite monochromatized Cu $K\alpha_1$ radiation, λ=0.154 06 nm), thermogravimetric/differential thermal analysis (TG/DSC, Pyres-1, USA), ultraviolet absorption (UV-3600, Japan), photoluminescence analysis (PL, F-2500, Japan) and Fourier transformation infrared absorption (FTIR, Nexus-870), respectively.

2 Results and discussion

The XRD and SEM characterization results in typical conditions are shown in Fig.1. From SEM images, it can be seen that the products obtained before and after calcination, are cantaloupe-like particles (Fig. 1a and 1d) or bunchiness rods (Fig.1b and 1e). The cantaloupe-like particles are composed of short nanorods with diameters ranging from several tens nanometers to over 100 nm. For the calcined product, the bunchiness rods are composed of small particles with a diameter ca. 15 nm (as shown in Fig.1e).

Fig.1c shows the XRD pattern of the uncalcined product. All of the diffraction peaks in this pattern can be indexed to orthormbic phase of cerium carbonate hydroxide ($CeOHCO_3$) (PDF No.41-0013). From the XRD pattern of the calcined product (Fig.1f), it can be concluded that this product is made up of cubic phase CeO_2. The CeO_2 lattice constant calculated from the XRD pattern is a=0.541 6 nm, which is in good agreement with the literature value (a=0.541 1 nm, PDF No. 75-0390). No diffraction peaks corresponding to $CeOHCO_3$ or other impurities present in the XRD pattern (Fig.1f), which suggests that the $CeOHCO_3$ has completely been transformed to CeO_2 through calcination.

The transformation of $CeOHCO_3$ was further studied by TG/DSC and FTIR. The TG analysis for the uncalcined product, as shown in Fig.2a (curve Ⅰ), indicates that the weight loss is ca. 20 % in the range of 250 to 300 ℃. This weight loss corresponds well to the molecular weight decrease (20.7%) from $CeOHCO_3$ to CeO_2. On the DSC curve (curve Ⅱ in Fig.2a), there is an endothermic peak centered at ca. 280 ℃. Correlating TG and DSC results, it can be concluded that an endothermic reaction with decomposition is involved in the transformation process from $CeOHCO_3$ to CeO_2[22]. Also, this transformation can be seen in the FTIR spectra (as shown in Fig.2b). On curve Ⅰ for the uncalcined product, the bands at 715 cm^{-1} and 860 cm^{-1} correspond to the inside and outside bending modes of C=O, respectively[23]. The bands at 1 417, 1 496 and 1 798 cm^{-1} originate from the vibrations of C=O or O-C-O[24~26]. The wide band at 3 449 cm^{-1} may result from the O-H stretching vibration of -OH groups or physical absorbed water[22]. On curve Ⅱ for the calcined product, the bands mentioned above weaken or disappear, but a typical Ce-O stretching band appears at *ca.* 400 cm^{-1}[27].

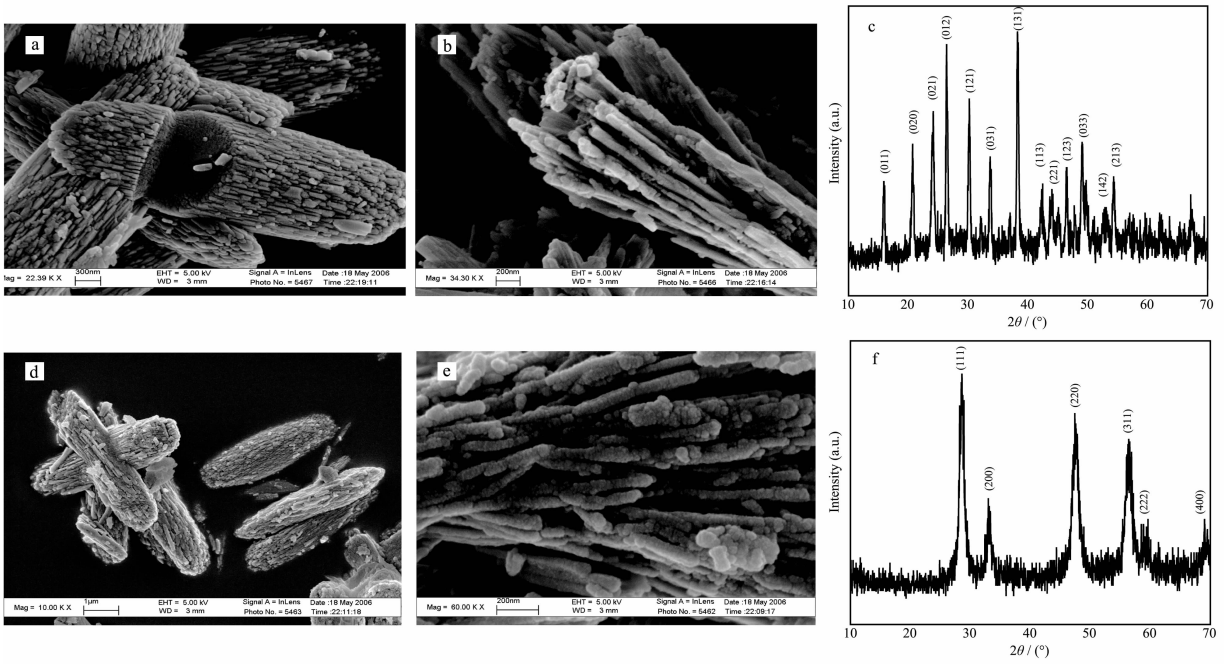

Fig.1 SEM and XRD characterization results: (a), (b) and (c) for the uncalcined product; (d), (e) and (f) for the calcined product

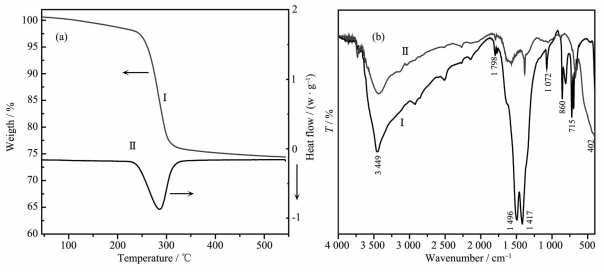

Fig.2 (a) Thermic analysis results of the uncalcined product: TG curve (curve Ⅰ) and DSC profile (curve Ⅱ);(b) FTIR spectra: curve Ⅰ (the uncalcined product); curve Ⅱ (the calcined product)

Based on the experiment results and literature reports[22,28~30], the possible reactions involved in synthesis process might be as follows:

$$CO(NH_2)_2 + 3H_2O \rightarrow 2NH_4^+ + 2OH^- + CO_2 \quad (1)$$

$$CO_2 + H_2O \rightarrow CO_3^{2-} + 2H^+ \quad (2)$$

$$Ce^{3+} + OH^- + CO_3^{2-} \rightarrow CeOHCO_3 \quad (3)$$

$$4CeOHCO_3 + O_2 \rightarrow 4CeO_2 + 2H_2O + 4CO_2 \quad (4)$$

The $CeOHCO_3$ microstructures are formed by nucleation and growth in solution with reaction (**3**), and the CeO_2 nanoparticles are obtained by calcining with reaction (**4**). During the nucleation and growth of $CeOHCO_3$, the CTAB in solution plays an important role in controlling reaction rate and seed growth direction[22]. As well known, the surfactant molecules are able to organize themselves into a variety of micelles, when their concentration reaches a critical value. These micelles affect the formation course of particles in solution. In our synthesis solution, large amounts of micelles are formed by the hydrophobic interaction of surfactant CTAB molecules. Since CTAB is completely ionized in aqueous solution, these micelles filled with alkyl chains bring along many positive charges in their polar shell[31,32]. The OH^- and CO_3^{2-} radicals, as the reaction radicals in the formation of $CeOHCO_3$, could be absorbed on the surface of the micelles by electrostatic force. Therefore, the nucleation of $CeOHCO_3$ and the formation of its microstructure, are controlled by CTAB micelles. As a result, little rods are first produced, and then the cantaloupe-like particles or bunchiness rods were formed by assembling rods under the function of CTAB micelles.

The function of CTAB was further studied by a series of experiments. It has been found that the block-like product was obtained if the CTAB concentration was decreased from 0.10 mol·L^{-1} (typical condition) to 0.05 mol·L^{-1}. The results show that the bunchiness rods are obtained only if the CTAB concentration is equal to or higher than 0.10 mol·L^{-1}. These phenomena imply that a high CTAB concentration solution, where a large

amount of micelles is formed, is essential for the formation of bunchiness rods. Fig.3 shows the XRD and SEM characterization results of the product obtained by hydrothermal synthesis. In this synthesis, the pr ecursors are the same as that in a typcal synthesis, except heating reaction solution in a Teflon-lined autoclave at 180 ℃ for 11 h. From Fig.3, it can be seen that the cubic phase CeO_2 block particles with diameter of 500~800 nm are obtained. Clearly, the morphology (large particles) of the hydrothermal product is different from that of the typical product. This morphology change may result from the destruction of CTAB micelles and the change of $CeOHCO_3$ growth mode in such a high temperature.

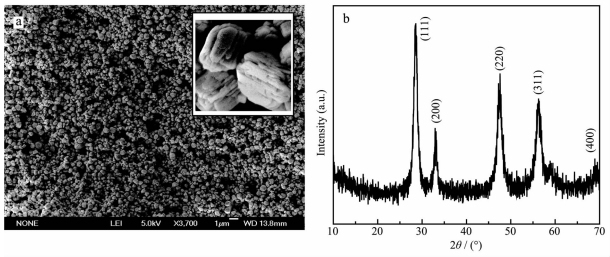

Peaks in XRD pattern can be all indexed to cubic phase CeO_2

Fig.3　Characterization results of the hydrothermal product: (a) SEM image; (b) XRD pattern

The optical properties of the typical products were determined at room temperature, and the results are shown in Fig.4. From the UV-Vis absorption spectra (Fig.4a), it can be seen that the absorption edge of CeO_2 is red-shifted relative to that of $CeOHCO_3$. With these absorption edges, the band gaps of the CeO_2 and $CeOHCO_3$ can be estimated as *ca.* 2.70 eV and 3.87 eV, respectively. For CeO_2, the strong UV absorption band at *ca.* 250~450 nm originates from the charge-transfer between the O2*p* and Ce4*f* states in O^{2-} and Ce^{4+}[27]. This absorption is much stronger than the $4f^1$-$5d^1$ transition absorption from the Ce^{3+} species[33], therefore, the absorption of $CeOHCO_3$ is weak in this wavelength range. According to the literature [34], the band gap of CeO_2 is 3.2 eV. Here, the band gap of our CeO_2 nanoparticles narrowed to 2.70 eV. As well known, the quantum size effect originating from the reduction of the particle size would give a band gap increase[35]. This novel reduction of our CeO_2 band gap is tentatively explained as follows. On the one hand, the close-congregation of the CeO_2 particles (as shown in Fig.1e) could intensively weaken the quantum size effect. On the other hand, the oxygen vacancies and defects of CeO_2 surface could further narrow the band gap. Here, it is worthy of pointing out that the CeO_2 with narrow band gap will have potential use in solar-cell due to its better response in the visible region of the solar spectrum.

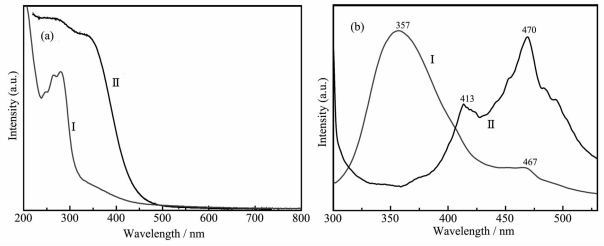

Fig.4　(a) UV-Vis absorption spectra of the $CeOHCO_3$ (curve Ⅰ) and CeO_2 (curve Ⅱ); (b) PL spectra (excited at 290 nm) of the $CeOHCO_3$ (curve Ⅰ) and CeO_2 (curve Ⅱ)

As shown in Fig.4b, the $CeOHCO_3$ produces a broad emission centered at *ca.* 360 nm (curve Ⅰ). This band may result from the fed transitions of Ce^{3+} between the $^2F_{5/2}$ ($4f^1$) ground state and the ^2D ($5d^1$) excited state[36]. Similarly, Han and his co-workers[37] have found the strong PL emission band at *ca.* 365 nm for orthormbic phase $CeOHCO_3$. According to the literature[38], the materials having such emission properties can be used as black-light materials for pest control. On the PL spectrum (curve Ⅱ) of the CeO_2 particles, there are two emission peaks centered at *ca.* 413 nm and 470 nm that can be attributed to the electron transition from different defect levels to O2*p* band[39,40]. The abundant defects in CeO_2 particles are important for fast oxygen transport and catalytic function[41].

3　Conclusion

In summary, the cantaloupe-like particles of $CeOHCO_3$ were synthesized in cetyltrimethylammonium bromide (CTAB) aqueous solution. The experimental results show that the high CTAB concentration plays an important role on the nucleation and formation of $CeOHCO_3$ microstructures. The orthormbic phase $CeOHCO_3$ as-formed can be transformed to cubic phase CeO_2 nanoparticles by calcination. By UV-Vis

absorption and photoluminescence analysis, it is found that the CeO_2 possess abundant defects, and the band gaps of the CeO_2 and $CeOHCO_3$ are *ca.* 2.70 eV and 3.87 eV, respectively.

References:

[1] Zhang J, Ju X, Wu Z Y, et al. *Chem. Mater.*, **2001**,**13**:4192~4197

[2] Sayle D C, Maicaneanu S A, Watson G W. *J. Am. Chem. Soc.*, **2002**,**124**:11429~11439

[3] Shao Z, Haile S M, Ahn J, et al. *Nature*, **2005**,**435**:795~

[4] Gu F B, Wang Z H, Han D M, et al. *Mater. Sci. Eng. B*, **2007**, **139**:62~68

[5] Messing G L, Zhang S C, Jayanthi G V. *Am. J. Ceram. Soc.*, **1993**,**76**:2707~2726

[6] Kosynkin V D, Arzgatkina A A, Ivanov E N, et al. *J. Alloys Compd.*, **2000**,**303**:421~425

[7] Patsalas P, Logothetidis S, Metaxa C. *Appl. Phys. Lett.*, **2002**, **81**:466~468

[8] Barbier J J, Oliviero L, Renard B. *Catal. Today*, **2002**,**75**:29~34

[9] Mori T, Drennan J, Wang Y R. *J. Therm. Anal. and Cal.*, **2002**, **70**:309~319

[10]Wang Z L, Feng X D. *J. Phys. Chem. B*, **2003**,**107**:13563~13566

[11]Wu L, Wiesmann H J, Moodenbaugh A R, et al. *Phys. Rev. B*, **2004**,**69**:125415~125423

[12]Arturas K, Prancis K V, Paulius P. *J. Crystal Growth*, **2007**, **304**:361~384

[13]Matijevic E, Has W P. *J. Colloid Interface Sci.*, **1987**,**118**: 506~523

[14]Hirano M, Kato E. *J. Am. Ceram. Soc.*, **1999**,**82**:786~790

[15]Han W Q, Wu L J, Zhu Y M. *J. Am. Chem. Soc.*, **2005**,**127**: 12814~12815

[16]Bonamartini A, Corradi F, Bondioli A M, et al. *Mater. Res. Bull.*, **2006**,**41**:38~44

[17]Tok A I Y, Boey F Y C, Dong Z, et al. *J. Mater. Proc. Tech.*, **2007**,**190**:217~222

[18]Raffaella L N, Roberta T, Graziella M, et al. *Chem. Mater.*, **2003**,**15**:1434~1440

[19]Dmitry G S, Rachel A C. *Chem. Mater.*, **2004**,**16**:2287~2292

[20]Aurélien V, Yuan Z Y, Du G H, et al. *Langmuir*, **2005**,**21**: 1132~1135

[21]Wu H P, Liu J F, Ge M Y, et al. *Chem. Mater.*, **2006**,**18**:1817~1820

[22]Wang S F, Gu F, Li C Z, et al. *Crystal Growth*, **2007**,**307**:386~394

[23]Sun C W, Sun J, Xiao G L, et al. *J. Phys. Chem. B*, **2006**,**110**: 13445~13452

[24]Vantomme A, Yuan Z Y, Du G, et al. *Langmuir*, **2005**,**21**(3): 1132~1135

[25]Xu J X, Li G S, Li L P. *Mater. Res. Bull*, (**2007**) **doi**:10.1016/j.materresbull. 2007.04.019

[26]Liang Y, Zhao J, Wang L. *J. Miner. Petrol.*, **2007**,**6**:12~16

[27]Chunman H, Jimmy C Y, Tszyan K, et al. *Chem. Mater.*, **2005**,**17**:4514~4522

[28]Chen S, Yu S H, Yu B, et al. *Chem. Eur. J.*, **2004**,**10**:3050~3058

[29]Wang C H, Lu H C. *Mater. Res. Bull.*, **2002**,**37**:783~792

[30]Guo Z Y, Du F L, Li G C, et al. *Inorg. Chem.*, **2006**,**45**:4167~4169

[31]Tornblom M, Henriksson U. *J. Phys. Chem. B*, **1997**,**101**:6028~6035

[32]Zhang S Y, Liu Y, Ma X, et al. *J. Phys. Chem. B*, **2006**,**110**: 9041~9047

[33]Murata T, Sato M, Yoshida H, et al. *J. Non-Cryst. Solids*, **2005**,**351**:312~316

[34]Orel Z, Orel B. *Physica Status Solidi B*, **1994**,**186**:K33~K36

[35]Corma A, Atienzar P, Garcia H, et al. *Nature Mater.*, **2004**,**3**: 394~397

[36]Pieterson L V, Reid M F, Wegh R T, et al. *Phys. Rev. B*, **2002**,**65**:045113~045128

[37]Han Z H, Guo N, Tang K B, et al. *J. Crystal Growth*, **2000**, **219**:315~318

[38]Han Z H, Qian Y T, Tang K B, et al. *Inorg. Chem. Commun*, **2003**,**6**:1117~1121

[39]Sun C W, Li H, Zhang H R, et al. *Nanotechnology*, **2005**,**16**: 1454~1463

[40]Chai C L, Yang S Y, Liu Z K, et al. *Chin. Sci. Bull*, **2003**,**48**: 1198~1200

[41]Sun C W, Li H, Chen L Q. *J. Phy. and Chem. Solids*, **2007**,**68**: 1785~1790